Advances in Science and Technology Research Journal

Advances in Science and Technology Research Journal 2022, 16(5), 202–215
https://doi.org/10.12913/22998624/154795
ISSN 2299-8624, License CC-BY 4.0

Received: 2022.08.13
Accepted: 2022.10.17
Published: 2022.11.01

Impact of T-Splitter on the Laminar Flow Field around Cylinder Pier

Rafi Mohammed Qasim[1], Safaa Hameed Faisal[1*], Tahseen Ali Jabbar[1]

[1] Basra Engineering Technical College, Southern Technical University, Basra, Iraq
* Corresponding author's e-mail: s_hfaisal100@stu.edu.iq

ABSTRACT
The hydrodynamic pattern, which surrounds the pier near a splitter that has T-shape, is investigated by adopting a numerical method and using ANSYS Fluent Software to achieve computation. The essential objective of this paper refers to revealing the behavior of the hydrodynamic field around the pier due to the existence of the upstream splitter plate. The T-splitter plate has not been used in previous works for controlling the flow field around the cylinder body. The main assumptions adopted in solving the hydrodynamic problem are incompressible, steady, and laminar flow. Reynolds number values are taken from 40 to 200 to guarantee laminar flow with laminar vortex street. The numerical investigation focuses on two main variables. These variables are the horizontal distance between the rear portion of a splitter and the pier center and bubble length. The numerical study comprises pressure contours, water velocity contours, and streamlines. Results reveal that bubbles are generated and developed due to the existence of the splitter. Four bubbles are generated, two of them are formed in the region between the splitter rear portion and pier leading portion and the other two bubbles are formed at the cylindrical pier wake region. The size and length of these four bubbles are dominated by the Reynolds number, these bubbles are non-symmetrical. It is revealed from the solution that with the rise in Reynolds number values then the disturbance will be increased simultaneously. The horizontal distance dominates the hydraulic response, which is described by the streamlines, pressure contours, and water flow contours. Furthermore, the Reynolds number has a significant influence on the pressure contours, water flow contours, and streamlines. Finally, a correlation equation is derived relying on bubble length, horizontal distance, and Reynolds number.

Keywords: bridge pier, hydraulic field; laminar flow, T- Splitter.

INTRODUCTION

The flow around the bridge piers takes more attention and concern by hydraulic designers. Many collapses occur due to the changing in the hydrodynamic pattern around the piers. The splitter is a structure that can be used to protect the bridge pier from hazards of high flow intensity. So, the splitter can be employed to reduce water velocity, water turbulence intensity, and scour depth around the pier respectively. The hydraulic pattern between the splitter and pier must be evaluated correctly to prevent any alteration or fluctuation in the hydrodynamic field. Several researchers are interested in this problem. Strykowski and Sreenivasan [1] performed experimental and numerical investigations on the vortex shedding formation and suppression respectively at low Reynolds numbers. A control cylinder is installed in a specified zone at the near-wake of the main cylinder. Based on this way, the vortex would be suppressed significantly and decrease its drag. Kwon and Choi [2] simulated the laminar vortex shedding at the rear of a circular cylinder and its control by placing a splitter plate in direct touch with the cylinder. It is found that vortex shedding disappeared completely when the splitter length becomes greater than the critical length. Also, the splitter length is proportional to the Reynolds number. Vortex shedding Strouhal number is decreasing rapidly when the plate length is increased. In addition, the splitter plate led to reducing the drag. Chen [3] employed the formulation of finite element

to investigate laminar flow separation around the cylinder bounded by two parallel plates. Furthermore, three different types of boundary conditions are studied. Hwang and Yang [4] studied numerically the drag reduction on a cylinder using splitter plates. The cylinder has a circular shape and the length of the two splitter plates is equal to the diameter of the cylinder. The first splitter plate is placed at the upstream of the cylinder while the second one is placed near the wake zone. It is found that the stagnation pressure is reduced by the upstream splitter plate while the base pressure is increased by the downstream splitter plate. Sen et al. [5] adopted stabilized finite-element method to investigate the laminar flow around the circular stationary cylinder in two dimensions. Reynolds number relies on stream velocity and cylinder diameter. The results are recorded for $6 \leq Re \leq 40$ and the blockages ratio between 0.000125 and 0.80. In addition, two different types of boundary conditions have been investigated at the sidewalls: towing tank and slip wall. Singha and Sinhamahapatra [6] analyzed numerically the flow past a cylinder, which is placed centrally into the flow channel. Also, the blockage ratio is adopted in the analysis. Simulation is done in a two-dimension with a low range of Reynolds numbers.

Sato and Kobayashi [7] did a numerical investigation to study the flow pattern around a cylinder with a circular shape that was put in a uniform flow. The investigation involved various phenomena that occurred with von Karman vortices. The hydraulic analysis is performed by Abaqus software. Noor et al. [8] implemented a numerical study to investigate the laminar flow across the circular when the Reynolds number is low. Passive control is employed in the study in which two rods are used. The first rod is located at the cylinder upstream while the second rod is located at the cylinder downstream. Both rods reduce a hydrodynamics force, which acts on the cylinder. Both rods importantly contribute to decreasing the drag and fluctuation lift compared with a cylinder without the presence of the rods. Khassaf and Obied [9] performed an experimental work using a guide panel on the local scour around the pier of the bridge. They discovered from the experimental results that when the height of the panel decreases then the scour depth will be decreased too. Yamini et al. [10] investigated numerically the scour around the pile of the offshore wind turbine. The study dealt with the combining both of waves and currents, also changing the bed materials type and changing the turbine substructure. The contrast in the wave height, current velocity, pile diameter, and bed particle size are considered in the numerical investigating. The splitter can be used to decrease the scour depth around hydraulic structures such as bridge piers, Abdulhussein et al. [11], performed an experimental work to study the influence of adopting the strip guide panel to decrease the scour depth around a pier which has a circular shape. They inferred from the experimental results that the depth of scour around the bridge pier nearby the strip panel is less compared with the depth of scour without a strip panel. Alizadeh et al. [12]. investigated numerically the possibility of drag force reduction on a rigid cylinder by adopting single and double horizontal plates. The lengths of the plates were equal to the diameter of the cylinder and were positioned along the horizontal centerline. They found that the upstream plate reduces the stagnation pressure, and the downstream plate rises the pressure behind the cylinder by eliminating vortexes.

Zhou et al. [13] investigated experimentally the influence of the splitter plate placed at the upstream of the circular cylinder. They found that when the plate is rigid, then the variation in Reynolds number with drag coefficient is similar to the case of cylinder without splitter. Also, when the plate length or Reynolds number increase, the flexible splitter plate is bent to the side due to the flow impact. Mishra et al. [14] investigate the control of the passive flow numerically. The flow around a circular cylinder is done in two dimensions. Here, the cylinder contains slit. The parameters slit angle and slit width ratio are substantial dominate the critical Reynolds number. They found that the pressure at the rear part of the cylinder increases due to additional quantity of discharge through the slit, which in turn leads to an increase in the critical Reynolds number of the modified cylinder. Gumgum and Guney [15] did an experimental study to discover the influence of sediment feeding around the pier of the bridge that have a circular cross section. Their experiment focused on live-bed scour under flood waves. Experiments are achieved first without feeding of sediment and the total load was collected at predetermined time intervals. Then the same experiments are achieved by adopting feeding with the same amount of collected sediment. Jabbar et al. [16], Qasim et al. [17], Qasim and

Jabbar [18] stated the effectiveness of the vane structure on the hydrodynamic field around cylinder like pier. The vane changes the hydrodynamic field significantly. Several variables are investigated numerically by using ANSYS Fluent. It is very important here to mention the vane will work like splitter plate.

The current study aim to:

a) Determine the relationship between ratio X and ratio η for Reynolds numbers ranging from 40 to 200 (The definitions of ratio X and ratio η can be found in the paper's next sections).
b) Determine the relationship between the ratio η and Reynolds number for the various values of ratio X (X = 0.5, 1, and 1.5).
c) Investigate the streamline for various values of ratio X. Here, Reynolds number values employed in the analysis are 40, 120, and 200.
d) Study the flow velocity and pressure for various values of Reynolds number and ratio X.
e) Obtain a correlation including Reynolds number, ratio X, and ratio η.

Actually, the suitable and reasonable parameters, which depend on studying the water hydrodynamic field around the pier or any obstacle, are velocity and pressure owing to inversely proportional between them. Therefore, this study deals with both of them, in addition, the study gives a distribution to the flow deformation by dealing with streamlines. Here, the pressure field around the pier was affected directly by the existence of the splitter plate, where the stagnation pressure points will transmit from the leading part of the pier to the leading part of the splitter plate. This issue will reflect on the pressure field around the pier and lead to a change in the values of flow velocity around the pier. In fact, the investigation gives an image of the hydraulic pattern that expected to occur around the pier owing to the existence of the splitter plate over a fixed, non-mobile bed (rigid bed) of the channel. The primary benefit of this investigation, give an approximate answer about the hydraulic pattern around the pier nearby the splitter plate over the fixed and mobile bed, like a river, where the splitter plate is placed upstream of the pier. Here, the splitter plate works to reduce the scour depth around the pier and works as a protection device in spite of the splitter plate has a direct impact on the sediment in the region around the pier.

METHODOLOGY

The entire hydraulic system adopted in this study is composed of a circular bridge pier, a T-splitter, and an incompressible water flow. Figure 1 shows a two-dimensional schematic illustration of the entire hydraulic problem. The water flow crosses the T-splitter from the left portion moving towards the circular pier. The water flow around the circular pier is deformed due to the presence of the splitter, which has a T-shape. The fluid size domain, which is adopted in two-dimensional analysis for solving the hydraulic interaction problem, is shown in Figure 2. Here, the T-splitter dimensions are taken as a function of pier diameter (all dimensions of the splitter are equal to the diameter of the pier except for the splitter thickness which is equal to 0.1 of the pier diameter). The position of the T-splitter is at the upstream region of the pier. The analysis depends on the location of X which is referred to the distance measured horizontally from T-splitter downstream to the center of the pier. This means that when $x = D/2$, the splitter has a direct touch with the boundary layer region of the pier. From Figure 1; L: is referred to

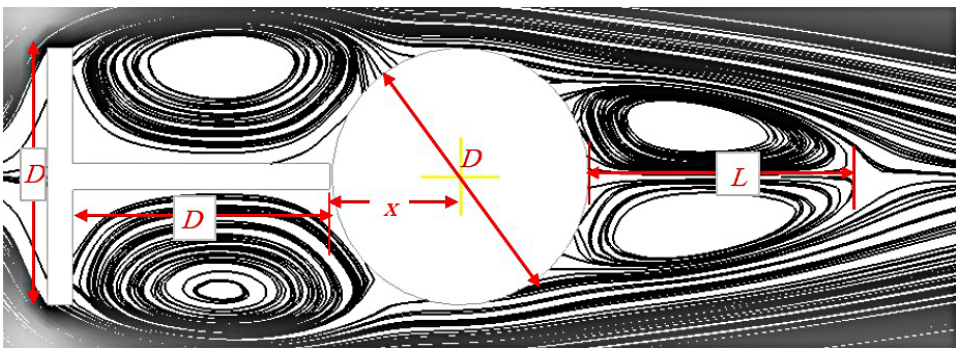

Figure 1. Hydraulic system problem (flow, T-splitter and Pier)

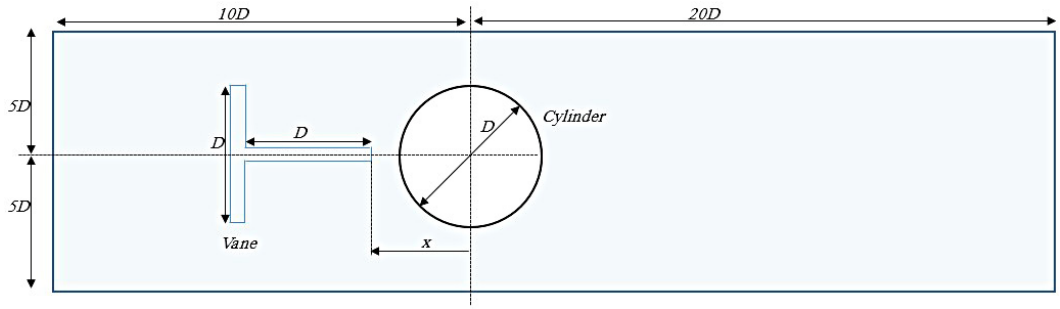

Figure 2. Problem size domain

the bubble length at the pier wake region (L=s). The hydraulic analysis is done for laminar flow where the Reynolds number values are from 40 to 200. In general, vortex street becomes laminar for Reynolds numbers range ($40 \leq Re \leq 200$) [19]. ANSYS Fluent software is used to solve the problem of steady flow field. Tables 1 and 2 illustrates water physical properties and the solution boundary conditions respectively.

The current paper focuses on two different non-dimensional ratios which are η and X. These two ratios are defined as:

$$\eta = \frac{s}{D} \tag{1}$$

$$X = \frac{x}{D} \tag{2}$$

where: s – bubble length, D – cylinder diameter.

The CFD governing equations that will be used for the simulation are the conservation of momentum equations (Eq. 3 and 4) and incompressible fluid continuity equation (Eq. 5) given below [20]. In general, fluids are incompressible, in this paper we use water as flow material and not air. In addition, the paper adopted laminar flow, in this case the flow velocity is relatively small. Therefore, there is no problem in assume the flow is an incompressible.

Table 1. Physical properties of water

Density (kg/m³)	Viscosity (kg/m·s)
997.1	89.05E-5

Table 2. Hydraulic problem boundary conditions

Location	Type
Inlet	Inlet velocity
Outlet	Outlet pressure
T-Splitter and pier	No-slip
Channel bed and sides	No-slip

$$u\frac{\partial u}{\partial x} + v\frac{\partial u}{\partial y} = -\frac{1}{\rho}\frac{\partial P}{\partial x} + \frac{\mu}{\rho}\left(\frac{\partial^2 u}{\partial x^2} + \frac{\partial^2 u}{\partial y^2}\right) \tag{3}$$

$$u\frac{\partial v}{\partial x} + v\frac{\partial v}{\partial y} = -\frac{1}{\rho}\frac{\partial P}{\partial y} + \frac{\mu}{\rho}\left(\frac{\partial^2 v}{\partial x^2} + \frac{\partial^2 v}{\partial y^2}\right) \tag{4}$$

$$\frac{\partial u}{\partial x} + \frac{\partial v}{\partial y} = 0 \tag{5}$$

Table 3 contain the total numbers of nodes and elements for different values of ratio x/D. Also, Figure 3 shows the mesh of the completely hydraulic system when $x/D = 1.2$.

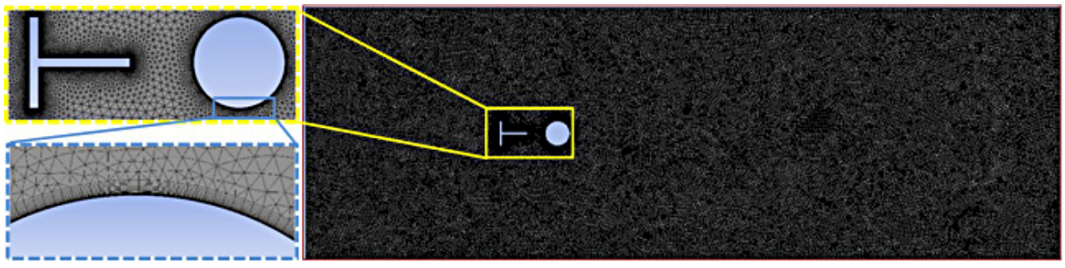

Figure 3. Mesh of hydraulic system for case x/D=1.2

Table 3. Details of nodes and elements for various values of x/D

x/D	Number of elements	Number of nodes
0.5	29926	30357
0.6	29948	30381
0.7	29946	30380
0.8	29915	30350
0.9	29970	30403
1	29912	30343
1.1	29927	30361
1.2	29939	30373
1.3	29913	30347
1.4	29941	30375
1.5	29909	30338

VALIDATION

The first step prior to performing the hydraulic analysis to discover the interference in flow field between the pier and T-splitter is to validate the current software code. The comparison is carried out for flow around cylinder in two dimensional fluid domain carried out by Rajani et al. [21]. Figure 4 clarify the relation between the flow separation angle and Reynolds numbers. The figure shows no variance in the previous result and current result.

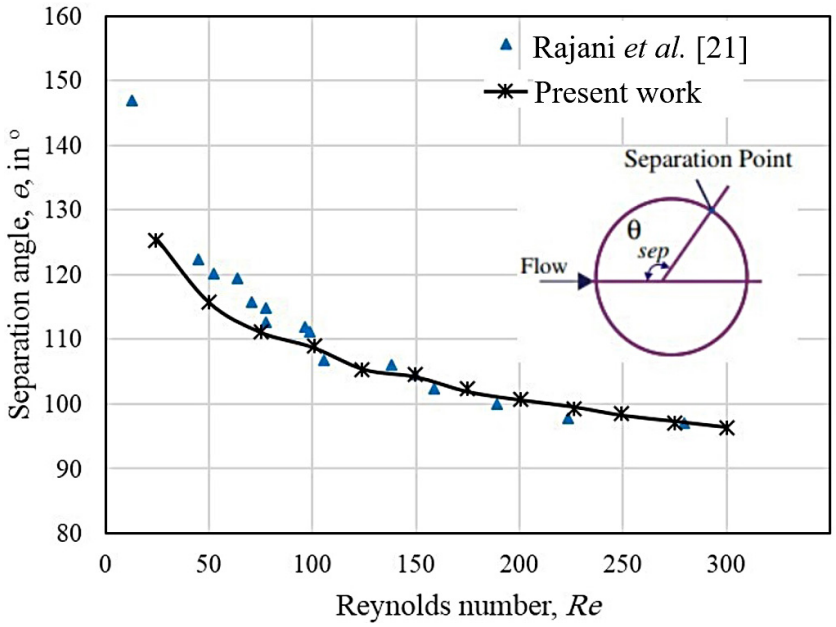

Figure 4. Relation between Reynolds number and separation angle

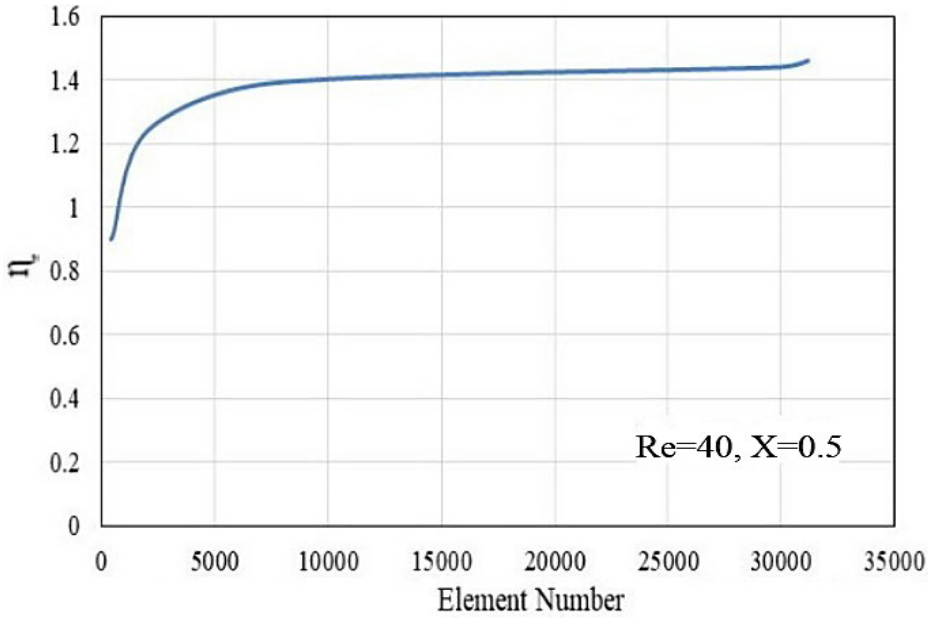

Figure 5. The adopted mesh independent

MESH INDEPENDENT

The number of elements has a significant impact on the flow field around both the splitter and the pier. It is critical to employ the correct number of elements to complete the solution. The relationship between the number of elements and the ratio η (case study from [22]) is shown in Figure 5, where η is the ratio between bubble length and cylinder diameter. When the number of elements exceeds 10000, the ratio remains constant, as seen in the Figure 5. It is generated when Re = 40 and T-splitter is in direct contact with the pier (X = 0.5).

RESULTS AND DISCUSSION

The hydrodynamic pattern around cylindrical bodies is considered a complex hydraulic problem due to the effect of body curvature on the flow which passes the body. This problem becomes more important when the body is nearby the splitter. Here, the interaction between two different hydrodynamic patterns will occur. The first pattern is around the cylindrical body and the second is around the splitter. The present paper deals with this subject. Figure 6a, Figure 6b, and Figure 6c reveal that with increasing the ratio X, then the ratio η will be decreased. In other words, when the distance between the splitter downstream and the center of the pier increases, the shortage of bubble length will happen in the wake region. This response occurs with the various Reynolds number values. In the wake region, bubble length will be affected directly by the Reynolds number. The instability in the wake region happens with an increase in Reynolds number values. In the case of the pier neighboring the splitter, separation points can be divided into two types; fixed and mobile points. The fixed points are located on the corners of the T-splitter while the mobile points are located on the circumference of the pier. Therefore, with an increase in the horizontal distance X, the alteration in the location of movable points along the perimeter of the pier will occur and this is reflected directly on the bubble length at the wake region. Reynolds number values against the ratio η is seen in Figure 7. With increasing Reynolds number, the ratio η will increased. The raise in Reynolds number lead to the bubble stretching at the wake zone. The separation points positions along the circular

a)

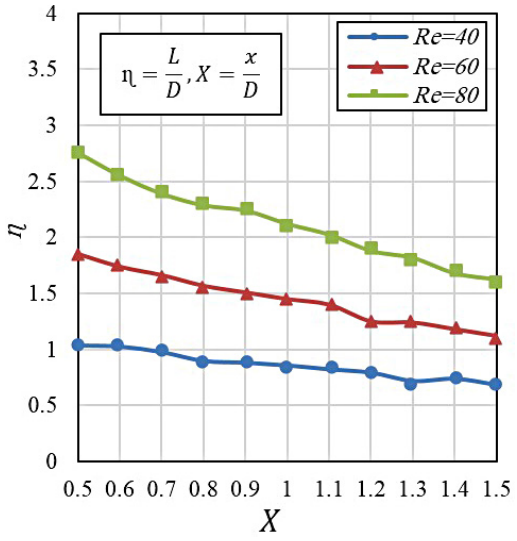

b)

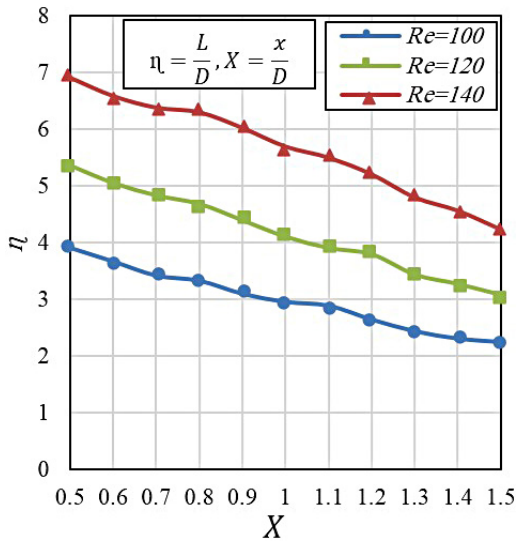

c)

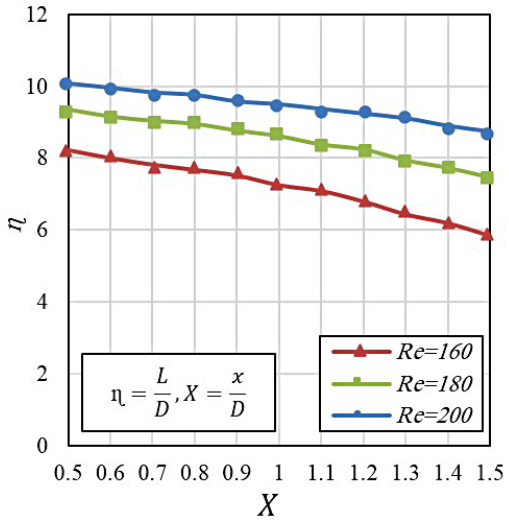

Figure 6. Relation between the ratio X and ratio η, for (a) 40 ≤ Re ≤8 0, (b) 100 ≤ Re ≤ 140, (c) 160 ≤ Re ≤ 200

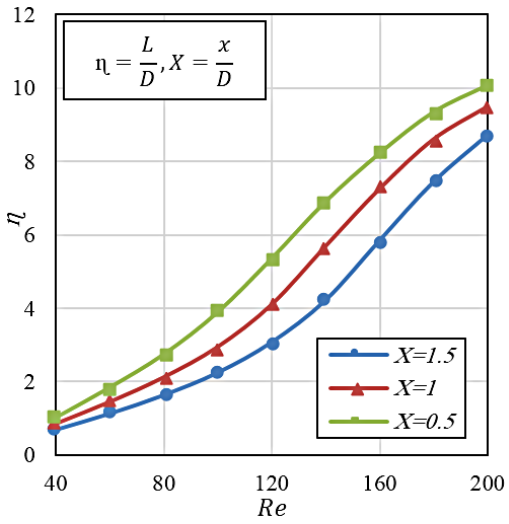

Figure 7. The effect of splitter position and Re on the ratio η

pier circumference are more affected by T-splitter existence and this will be effected on the bubble extension. It is apparent from Figure 7 that there is a nonlinear trend in the relationship between Re and ratio η.

Streamline contours are shown in Figure 8a, Figure 8b, and Figure 8c considering various values of the ratio X at Re = 40. For different values of the ratio X, streamline contours reveal a noticeable bubble that generates and develops at the wake region for the pier. The figures show a pair of non-symmetrical bubbles that generated and developed in the wake region. However, an interesting phenomenon will happen, which is the formation of non-symmetrical pair of bubbles in the zone between the rear portion of the T-splitter and in the front portion of the pier. These bubbles will grow regardless of the horizontal distance between the pier center and the rear portion of the splitter. The size of the upstream bubbles is greater than the downstream bubbles. Also, the upstream bubbles become larger in size with the increase in the horizontal distance and this behavior is not shown for downstream bubbles.

The flow becomes unstable with the increase in the Reynolds number. This means an increase in disturbance and this led to a change in the size of the bubble regardless of the bubble's position and ratio X. This appears clearly in Figure 9 and Figure 10.

For Figure 9, with the increase in ratio X, the bubbles in the wake region become shorter or shrink while the bubbles between the leading portion of the pier and the rear portion of the splitter become larger in size and move toward the sides of the pier. All bubbles are non-symmetrical. For Figure 10, the bubbles become thinner and more elongated and this happens due to rising in the value of the Reynolds number which leads to instability in the flow field.

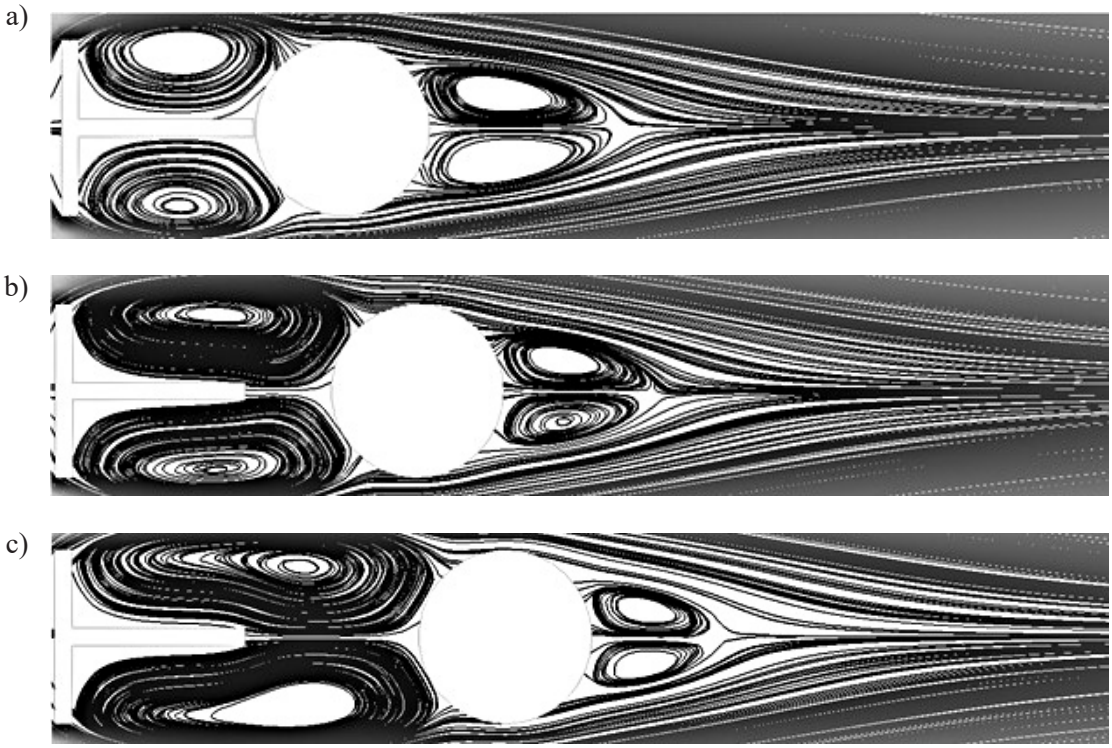

Figure 8. Streamlines at (a) Re = 40, X = 0.5; (b) Re = 40, X = 1; Re = 40, X = 1.5

Figure 9. Streamlines at (a) Re = 120, X = 0.5; (b) Re = 120, X = 1; Re = 120, X = 1.5

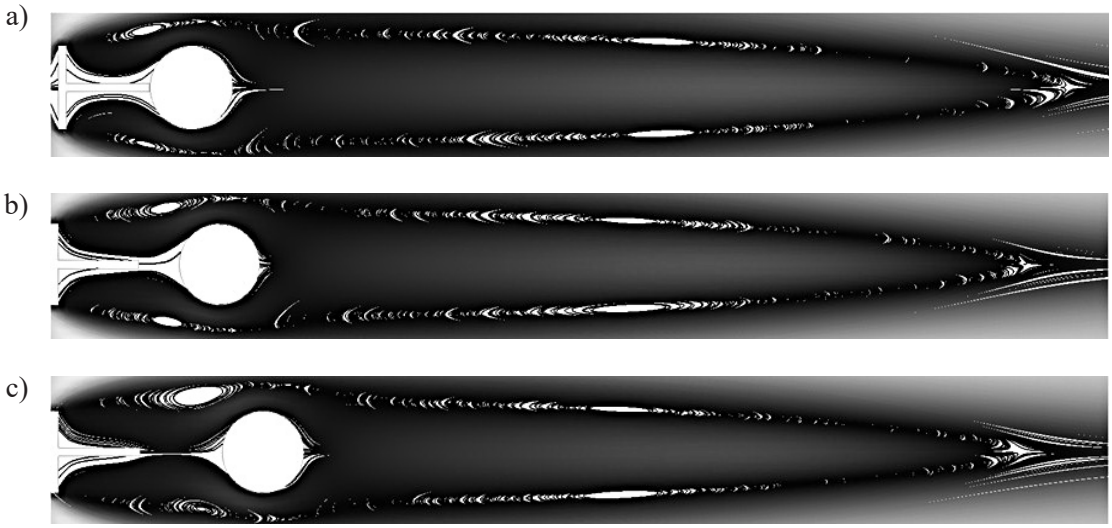

Figure 10. Streamlines at Re = 200, X = 0.5; (b) Re = 200, X = 1; Re = 200, X = 1.5

Figure 11 reveals the pressure and velocity contours respectively at Re=40 for various values of the ratio X.

The T-splitter existence causes a change in the pressure distribution around the circular pier. The pressure distribution begins with positive values at the leading portion of the T-splitter and then changes to negative values that begin with the rear portion of the T-splitter and move toward the leading portion of the circular pier and expands until the wake zone of the pier. This behavior is shown for all values of the ratio X, only when X = 1.5, the negative pressure will be surrounding the pier completely. At X = 0.5, the maximum positive pressure value at the leading part of the splitter is equal to 0.0147 Pa and equal to 0.0148 Pa when X = 1, also when X = 1.5 the pressure is equal to 0.015 Pa. It is shown a sensitive increase in positive pressure values with an increase in the ratio X, commonly the presence of the splitter shifted the stagnation point from the leading portion of the pier to the leading portion of the splitter. This transformation causes a reduction in stagnation pressure in the region between the splitter and pier, as well as increases pressure at the leading portion of the splitter. The negative pressure will increase as we move from the rear portion of the splitter toward the leading part of the pier. With the increase

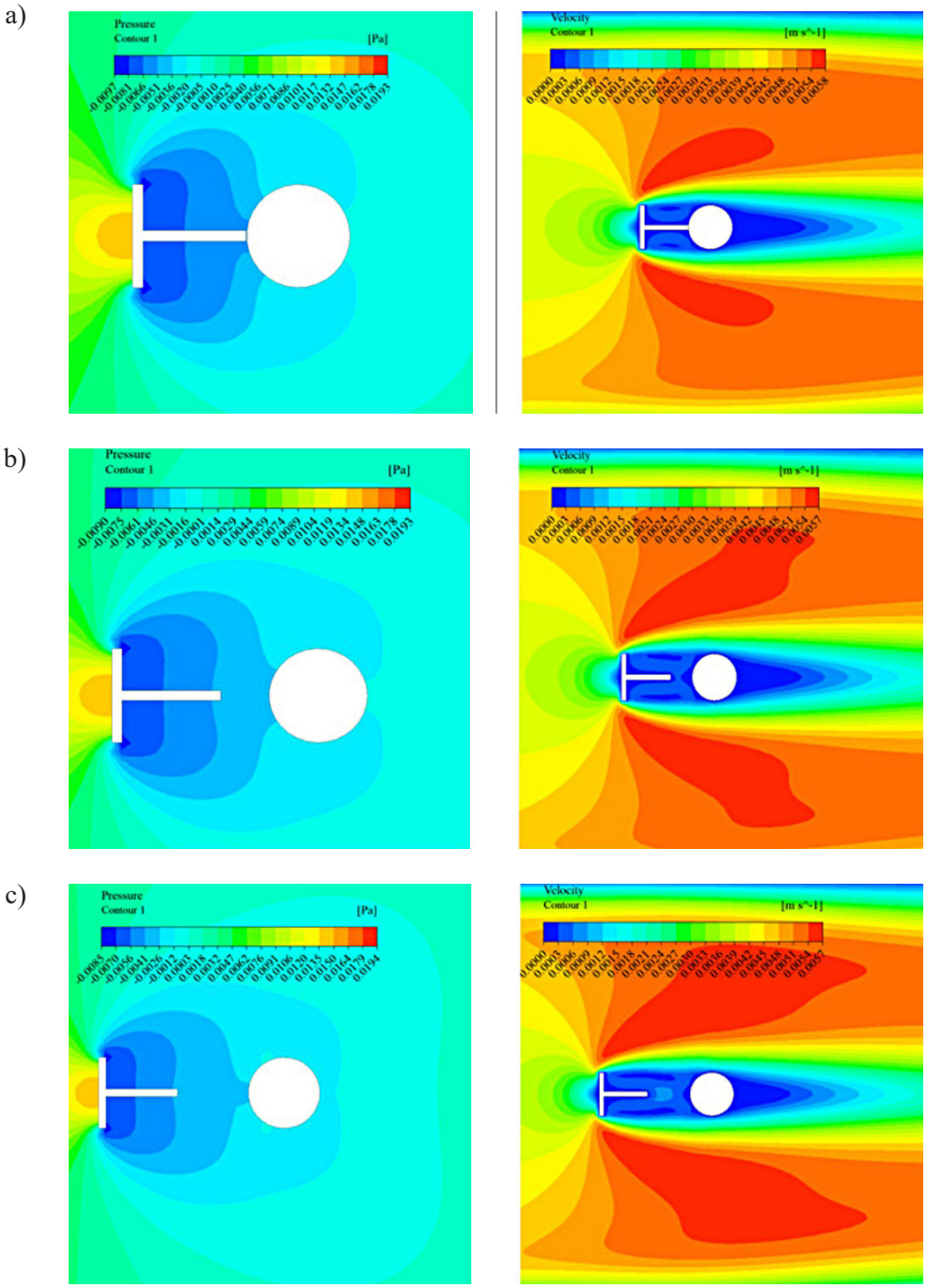

Figure 11. The pressure and velocity contours at (a) Re = 40, X = 0.5; (b) Re = 40, X = 1; (c) Re = 40, X = 1.5

in Reynolds number, the positive pressure will be raised and this is shown clearly in Figure 12 and Figure 13. At Reynolds number equal to 120, for positive pressure when $X = 0.5$, the maximum value at the leading part of the splitter is equal to 0.1086 Pa and equal to 0.1077 Pa when $X = 1$, also when $X = 1.5$ the pressure is equal to 0.1073 Pa. While at Reynolds number equals to 200, for positive pressure when $X = 0.5$, the maximum value at the leading part of the splitter is equal to 0.3049 Pa and equal to 0.3026 Pa when $X = 1$, also when $X = 1.5$ the pressure is equal to 0.2994Pa.

Figures 11, 12, and 13, show the flow velocity contours at $Re = 40$, $Re = 120$, and $Re = 200$ respectively for different values of the ratio X. Referring to velocity contours, the flow velocity magnitude around the T-splitter nearby the pier is smaller than the flow velocity magnitude in the remaining area of the region when we move laterally toward the boundary of the fluid domain. The flow velocity is affected by the flow separation and flow dissipation, the water velocity suffers from massive alteration in magnitude, because of separation and dissipation processes that happen along the splitter perimeter.

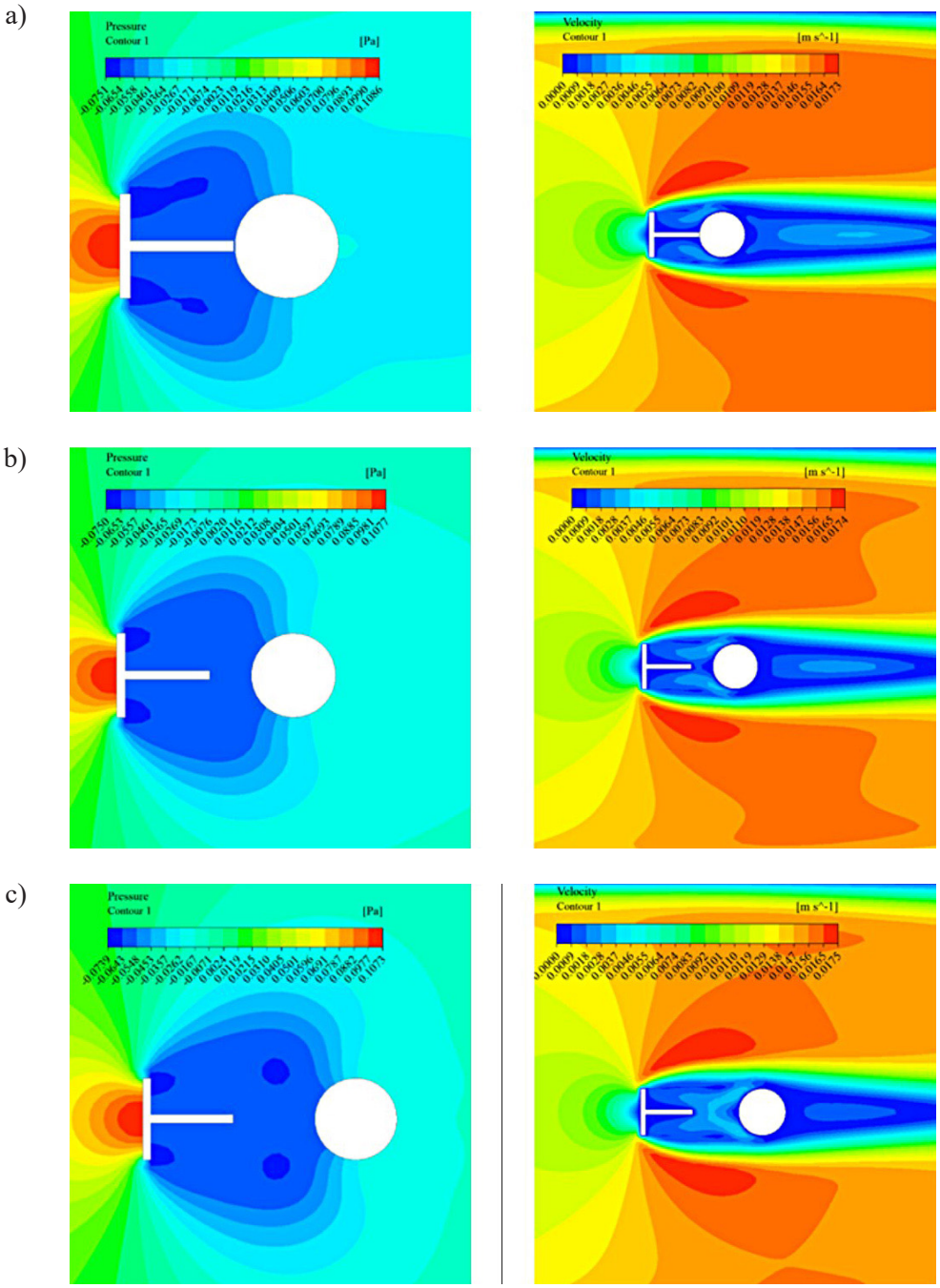

Figure 12. The pressure and velocity contours at (a) Re = 120, X = 0.5; (b) Re = 120, (c) X = 1; Re = 120, X = 1.5

A correlation that relies on the numerical solution is derived to link the ratio η as a function of the Reynolds number and the ratio X. This equation is considered nonlinear with with $R^2 = 0.986$. It is given by:

$$\eta = A\, Re^B\, X^C = \\ = 0.01406 Re^{1.177} X^{-0.4109} \tag{6}$$

Applicable for:

$$40 \leq Re \leq 200 \text{ and } 0.5 \leq X \leq 1.5$$

Comparative study

The flow around bridge pier nearby T-splitter has not been investigated in the previous works, so it is difficult to make a comparison study between this study and any previous study. However, we adopt the following procedure to make a comparison study. First, we perform a comparison between the results obtained from the previous studies for the flow around cylinder with Re = 15 ([23] and [5]) and the current study with the same Reynolds number. Figure 14

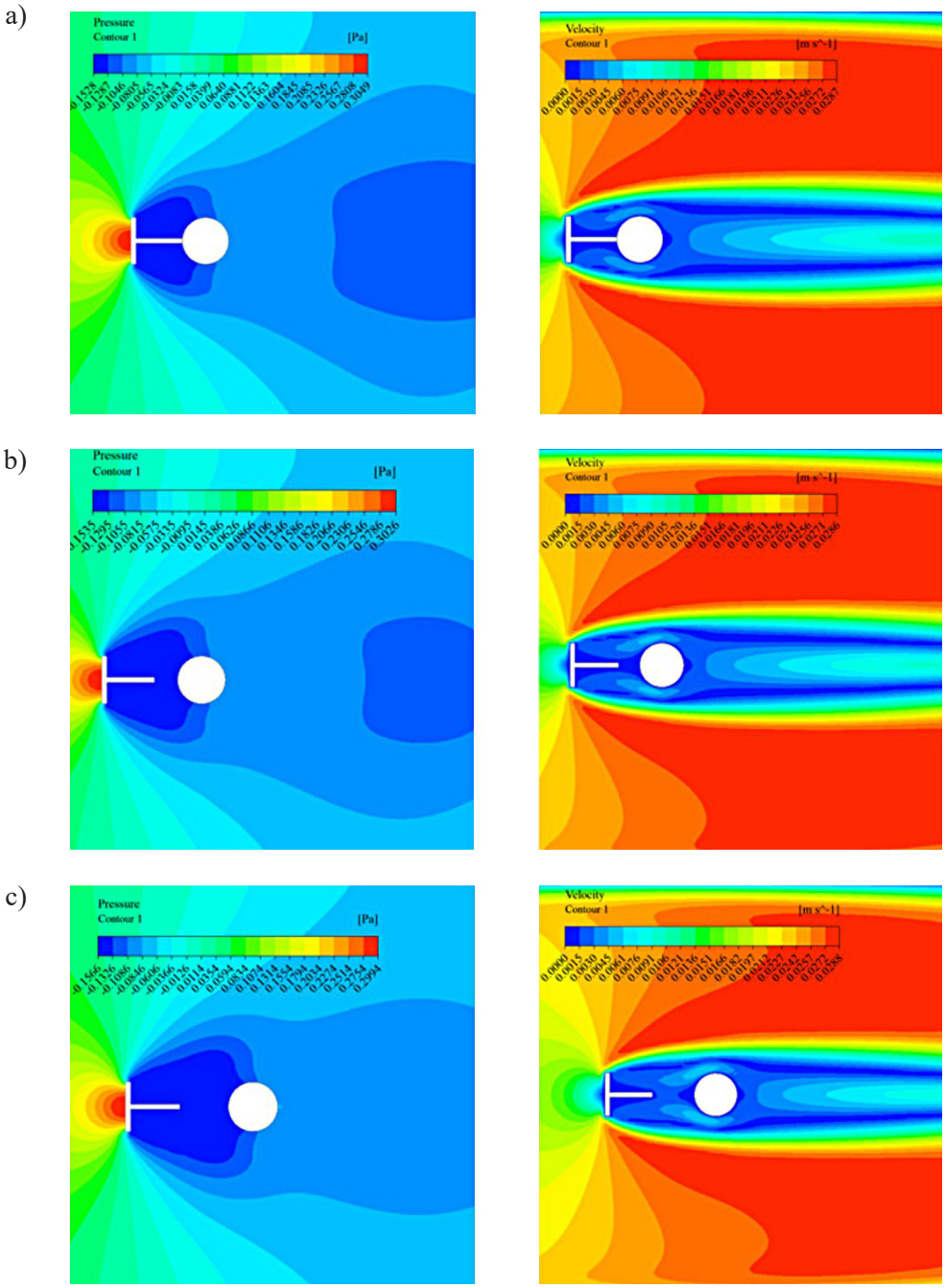

Figure 13a. The pressure and velocity contours at (a) Re = 200, X = 0.5; (b) Re = 200, X = 1; (c) Re = 200, X = 1.5

shows the relation between coefficient of pressure and the angle θ for Re = 15. It is clear from figure that excellent agreement is appeared from the comparison. Here, there is no contrast in the obtained results between the previous studied and the current study. The previous studied were performed in two dimensions flow with steady and laminar flow. Furthermore, Figure 15 shows the comparison between the previous studies and the current study with and without T-splitter plate for the relation between pressure coefficient and the angle θ, it is obvious from figure the contrast in the result is appeared owing to the transmission of the forward stagnation point from the leading part of the cylinder to the leading part of the splitter plate. Now we deal with figure 16 which is display clearly the relation between pressure coefficient and the angle θ for the current study, figure give a comparison between flow field around cylinder without and with splitter plate. When the angle less than 60 degree, the pressure coefficient of alone cylinder

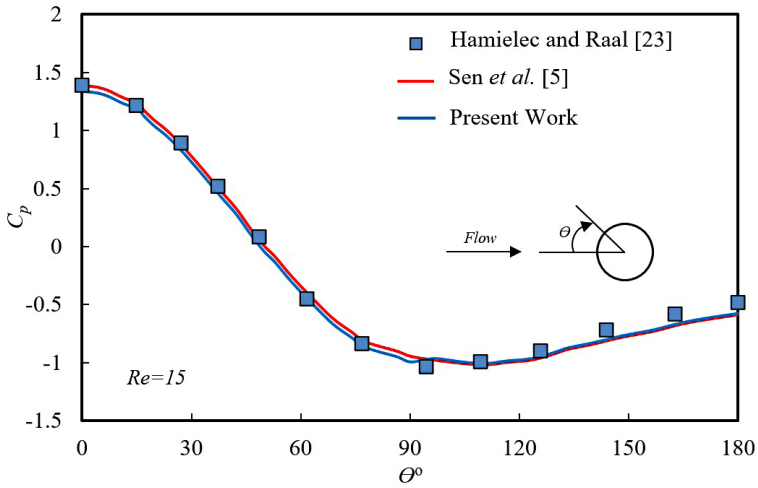

Figure 14. Relation between pressure coefficient and the angle θ at Re = 15 without splitter

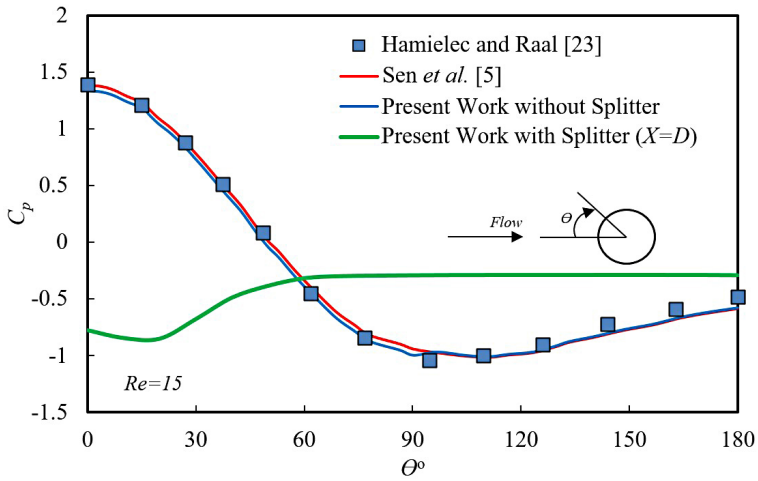

Figure 15. Relation between pressure coefficient and the angle θ at Re = 15 with and without splitter

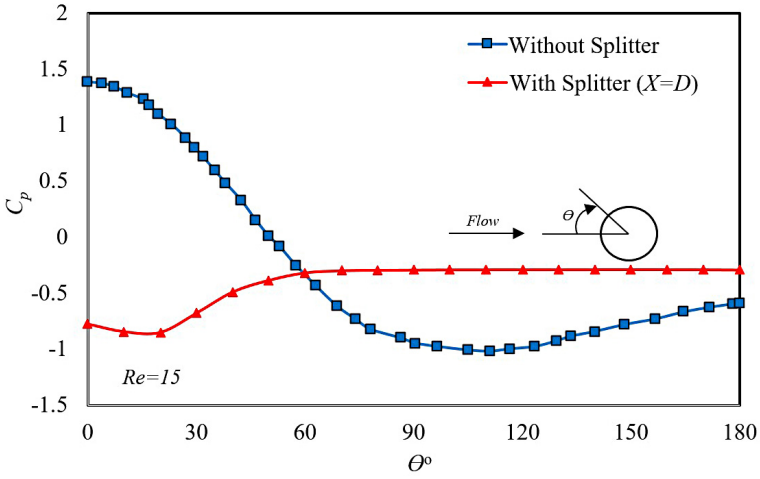

Figure 16. Relation between pressure coefficient and the angle θ at Re=15 without and with splitter for X=D

begin from high value and drop gradually, while for cylinder nearby splitter, the pressure coefficient begin from low value and rise gradually. At angle 60 degree, both curves are intersected. After angle 60 degree the curve for alone cylinder continue to drop gradually, while the curve for a cylinder nearby splitter approximately become line (linear trend).

CONCLUSIONS

The aim of the numerical investigating was to find a detailed description of the hydrodynamic pattern around pier nearby T-splitter plate. Then to study the effect of the upstream splitter plate on the pressure field, velocity field and streamlines. First, the existence of a T-splitter caused a significant change in the disturbance in the wake region, pressure field, velocity field and streamlines.The flow disturbance mainly relies on the Reynolds number. Here, Reynolds number has a major influence on the pressure field, velocity field and streamlines. The current simulation concentrates on the bubbles' size and length. Reynolds numbers values has major effect on the bubbles' size and length. Here, the bubble's size and length rely on the distance between the rear portion of a T-splitter and the pier center. Also, from numerical simulation, we infer that the horizontal distance and Reynolds number have a direct impact on bubbles formation and grow, especially those bubbles which are generated and grow in the zone between the leading portion of the pier and the rear portion of a T-splitter. Furthermore, the presence of a T-splitter will contribute to the changing of pressure values from positive to negative. In addition, the wake region of the cylindrical pier relies on Reynolds number values. Here, we must mention to the challenges and difficulties in select the configuration and shape of the splitter plate. The selection depends on how many processes which happens along the wetted perimeter of splitter plate. For T-splitter two different processes will occur along the wetted perimeter and these processes are flow separation and flow dissipation. It is recommended to repeat the same work in three dimensions hydraulic analysis, or/and considering different size for pier and splitter plate.

REFERENCES

1. Strykowski P.J., Sreenivasan K.R. On the formation and suppression of vortex shedding at low Reynolds numbers. Journal of Fluid Mechanics. 1990; 218(1): 71–107. https://doi.org/10.1017/s0022112090000933
2. Kwon K., Choi H. Control of laminar vortex shedding behind a circular cylinder using splitter plates. Physics of Fluids. 1996; 8(2): 479–486. https://doi.org/10.1063/1.868801
3. Chen J.H. Laminar separation of flow past a circular cylinder between two parallel plates. Proc. Natl Sci. Counc. ROC A. 2000; 24: 341–351.
4. Hwang J-Y., Yang K-S. Drag reduction on a circular cylinder using dual detached splitter plates. Journal of Wind Engineering and Industrial Aerodynamics. 2007; 95(7): 551–564. https://doi.org/10.1016/j.jweia.2006.11.003
5. Sen S., Mittal S., Biswas G. Steady separated flow past a circular cylinder at low Reynolds numbers. Journal of Fluid Mechanics. 2009; 620: 89–119. https://doi.org/10.1017/s0022112008004904
6. Singha S., Sinhamahapatra K.P. Flow past a circular cylinder between parallel walls at low reynolds numbers. Ocean Engineering. 2010; 37(8–9): 757–769. https://doi.org/10.1016/j.oceaneng.2010.02.012
7. Sato M., Kobayashi T. A fundamental study of the flow past a circular cylinder using Abaqus/CFD. SIMULIA Community Conference 2012.
8. Noor D.Z., Widiyono E, Suhariyanto, Rusdiyana L., Sarsetiyanto J. Laminar flow past a circular cylinder: Reduction of drag and fluctuating lift using upstream and downstream rods. Applied Mechanics and Materials. 2014; 493: 9–14. https://doi.org/10.4028/www.scientific.net/amm.493.9
9. Khassaf S. I, Obied N. A. Experimental study: bridge pier protection against local scour using guide panels. IOP Conference Series: Materials Science and Engineering. 2018; 433: 012006. https://doi.org/10.1088/1757-899x/433/1/012006
10. Yamini O. A., Mousavi S.H., Kavianpour M.R., Movahedi A. Numerical modeling of sediment scouring phenomenon around the offshore wind turbine pile in marine environment. Environmental Earth Sciences. 2018; 77(23): 1–15. https://doi.org/10.1007/s12665-018-7967-4
11. Abdulhussein I. A., Qasim R. M., Al-Asadi K. Pier scouring reduction using a strip guide flow panel device. RUDN Journal of Engineering Researches. 2019; 20(3): 229–235. https://doi.org/10.22363/2312-8143-2019-20-3-229-235
12. Alizadeh A, Jafarmadar S, Jebrail Zekri H. Use of one and two horizontal plates to reduce the drag force on the rigid cylinder located inside the channel: approach of the immersed interface method. Advances in Science and Technology Research Journal. 2019; 13(4): 188–193. doi:10.12913/22998624/111803.
13. Zhou X., Wang JJ, Hu Y. Experimental investigation on the flow around a circular cylinder with upstream splitter plate. Journal of Visualization. 2019; 22(4): 683–695. https://doi.org/10.1007/s12650-019-00560-x
14. Mishra A., Hanzla M., De A. Passive control of the onset of vortex shedding in flow past a circular cylinder using slit. Physics of Fluids. 2020; 32(1): 013602. https://doi.org/10.1063/1.5132799

15. Gumgum F., Guney M.S. Effect of sediment feeding on live-bed scour around circular bridge piers. Civil Engineering Journal. 2021; 7(5): 906–914. https://doi.org/10.28991/cej-2021-03091699
16. Jabbar T.A., Qasim R.M., Mohammed B.A. The impact of the vane angle on the hydraulic behaviour around the cylinder. In: International Multi-Disciplinary Conference-Integrated Sciences and Technologies, Sakarya, Turkey 2021. https://doi.org/10.4108/eai.7-9-2021.2315298
17. Qasim R.M., Jabbar T.A., Abdulhussein I.A., Flow field simulation between angle vane and cylinder. In: International Multi-Disciplinary Conference-Integrated Sciences and Technologies, Sakarya, Turkey 2021. https://doi.org/10.4108/eai.7-9-2021.2315181
18. Qasim, R.M., Jabbar, T.A., An analytic study of the effect of a vane on the hydraulic field around a cylinder. Incas Bulletin, 2021; 13(3): 123–139. https://doi.org/10.13111/2066-8201.2021.13.3.11
19. Sumer B.M., Fredsoe J. Hydrodynamics around cylindrical structures (revised edition). World Scientific, 2006.
20. Dahkil S. F., Gabbar T. A., Jaber D. K. Numerical study of the initial pressure and diameters ratio effect on the jet ejector performance. Basra Journal of Engneering Sciences. 2014; 14(1): 122–135.
21. Rajani B. N., Kandasamy A., Majumdar S. Numerical simulation of laminar flow past a circular cylinder. Applied Mathematical Modelling. 2009; 33(3): 1228–1247. https://doi.org/10.1016/j.apm.2008.01.017
22. Sharma B., Barman R. N. Steady laminar flow past a slotted circular cylinder. Physics of Fluids. 2020; 32(7): 073605. https://doi.org/10.1063/5.0007958
23. Hamielec A. E., Raal J. D. Numerical studies of viscous flow around circular cylinders. Physics of Fluids. 1969; 12(1): 11–17.